A Path Flux Analysis Method for the Reduction of Detailed Chemical Kinetic Mechanisms

Wenting Sun[1], Zheng Chen[2], Xiaolong Gou[3], Yiguang Ju[1]

[1] Department of Mechanical and Aerospace Engineering, Princeton University, Princeton, NJ 08544, USA

[2] State Key Laboratory for Turbulence and Complex Systems, College of Engineering, Peking University, Beijing 100871, China

[3] School of Power Engineering, Chongqing University, Chongqing 400044, China

Corresponding Author

Yiguang Ju

Mechanical and Aerospace Engineering

Princeton University

Princeton, NJ 08544, USA

Phone: +1-609-258-5644

Fax: +1-609-258-6233

Email: yju@princeton.edu

Keywords: PFA; Chemical kinetic mechanism; Reduced chemistry; n-decane; n-heptane

A Path Flux Analysis Method for the Reduction of Detailed Chemical Kinetic Mechanisms

Wenting Sun[1], Zheng Chen[2], Xiaolong Gou[3], Yiguang Ju[1]

[1] Department of Mechanical and Aerospace Engineering, Princeton University, Princeton, NJ 08544, USA

[2] State Key Laboratory for Turbulence and Complex Systems, College of Engineering, Peking University, Beijing 100871, China

[3] School of Power Engineering, Chongqing University, Chongqing 400044, China

Abstract

A direct Path Flux Analysis (PFA) method for kinetic mechanism reduction is proposed and validated by using high temperature ignition, perfect stirred reactors, and steady and unsteady flame propagations of n-heptane and n-decane/air mixtures. The formation and consumption fluxes of each species at multiple reaction path generations are analyzed and used to identify the important reaction pathways and the associated species. The formation and consumption path fluxes used in this method retain flux conservation information and are used to define the path indexes for the first and the second generation reaction paths related to a targeted species. Based on the indexes of each reaction path for the first and second generations, different sized reduced chemical mechanisms which contain different number of species are generated. The reduced mechanisms of n-heptane and n-decane obtained by using the present method are compared to those generated by the direct relation graph (DRG) method. The reaction path analysis for n-decane is conducted to demonstrate the validity of the present method. The comparisons of the ignition delay times, flame propagation speeds, flame structures, and unsteady spherical flame propagation processes showed that with either the same or significantly less number of species, the reduced mechanisms generated by the present PFA are more accurate than that of DRG in a broad range of initial pressures and temperatures. The method is also integrated with the dynamic multi-timescale method and a further increase of computation efficiency is achieved.

Introduction

Numerical simulation plays an increasingly important role in the study of combustion as a complementary or even replacement tool of the traditional, high-cost experiments for both scientific discoveries and engineering designs. However, combustion of fossil fuels involves hundreds of species and thousands of reactions and the employment of large detailed mechanisms in numerical simulation demands huge amount of CPU time. Although the available computational power is growing rapidly, a direct numerical simulation of turbulent combustion of hydrocarbon fuels with a detailed chemical kinetic mechanism at practical engine conditions remains challenging. Therefore, in order to make the numerical simulation of reactive flow computationally affordable and comprehensively accurate, the development of computational approaches for rigorous reduction of detailed mechanisms is essential.

Various mechanism reduction methods have been proposed to generate a reduced kinetic mechanism. The first approach is the sensitivity and rate analyses [1-3]. Although this method is very effective, it provides neither the timescales of different reaction groups nor the possible quasi-steady state (QSS) and partial equilibrium groups without good human experience. The second approach is the reaction Jacobian analysis which includes the Computational Singular Perturbation (CSP) method [4-6] and the Intrinsic Low Dimensional Manifold (ILDM) [7]. The CSP method obtains eigen-values and eigen-vectors of independent reaction modes, so that the fast and slow modes can be ranked by using the eigen-values. In the ILDM method, the low dimensional manifold is identified based on the decomposition of the Jacobian matrix of the chemical source term with the constraints of element and enthalpy conservations. Although these approaches can effectively identify the timescales of different reaction groups and the QSS species, it requires significant computation time to conduct Jacobian decomposition and mode projection and is significantly more complicated to implement. To achieve efficient calculations

of fast mode species, a third approach, the parameterization method, was proposed [8-11]. One example is the In-Situ Adaptive Tabulation (ISAT) [8]. The basic idea of ISAT is to integrate the chemical source term and store the information in a binary tree data structure as the simulation is being performed in-situ. ISAT is efficient if the flame structures are close to those created in the tabulated database. However, for non-premixed turbulent combustion involving a large kinetic mechanism with a broad temperature and concentration gradient distributions, time consumption in table buildup and the difficulties in data retrieval from a high dimensional table lookup lead to reduced advantage of ISAT in comparison to direct integration [12]. The fourth method is to use the reaction-rate or reaction path relations as a measure of the degree of interaction among species. The advantages of this kind of method are simple and fast, requiring minimal user interaction with the reduction process. Bendsten et al. [13] adopts the reaction matrix with each of whose elements P_{ij} defined as the net production rate of species i from all reactions involving j to establish a reduced reaction pathway (or mechanism). The set of important species is selected by going through the reaction matrix following the reaction path that connects one species to another that is most strongly coupled with it. The reduced mechanism is then completed by including a number of reactions such that for each of the selected species, a certain percentage of the total production or consumption rate (threshold value) of that species is kept in the reduced mechanism. Similar selection procedures are used in Directed Relation Graph (DRG) method [14, 15] and Directed Relation Graph method with Error Propagation (DRGEP) [16] by using the absolute and net reaction rates, respectively. However, the use of absolute reaction rates in DRG makes the relation index not conservative (the interaction coefficient or relation index is the ratio of species flux). DRGEP [16] employed the absolute net reaction flux to include error propagation across multi-generations. However, for the indirect relations, DRGEP only pick up the strongest reaction path which cannot identify the species flux physically when the intermediate species are more than one in parallel. Moreover, another problem of DRGEP is that

the definition of the interaction coefficient fails to identify the relation between the species that have both fast production and consumption rate, such as species having catalytic effect. A typical example is the NO_x catalytic effect on ignition enhancement [17], in which NO_x plays a role of catalyst and has a small net reaction rate but contributes significantly to the acceleration of ignition delay time. Another example is that a reaction path which has very long reaction chains with equal reaction rates. The definition of interaction coefficient of DRGEP may also be problematic [18]. In order to improve the accuracy of DRG and DRGEP method, a combination of DRG or DRGEP with species sensitivity was adopted [18, 19]. Unfortunately, the addition of sensitivity analysis is very computationally expensive. Furthermore, all the above methods are based on the analysis of one-generation direct flux/reaction rates. In order to improve the prediction of reaction fluxes, a multi-generation flux analysis including both consumption and production pathways are needed.

In this paper, we developed a Path Flux Analysis (PFA) method based on multi-generation fluxes to reduce the detailed chemical kinetic mechanism with improved model reduction accuracy compared to DRG method with the same size of a reduced mechanism. At first, the methodology of the PFA method is presented and analyzed. The method are tested by the simulations of ignition delay time of homogeneous mixtures, the extinction curves in a perfectly stirred reactor (PSR) and compared with the results of DRG and detailed mechanism. Then the reaction path analyses are conducted for n-decane and methane ignition problem with the NO_x catalytic effect to validate the method. The accuracy of the present model is also demonstrated by comparing the steady and unsteady flame propagation speeds and structures with those of DRG and the detailed mechanism. Finally, the reduced mechanism is integrated with the Hybrid Multi-Time Scale (HMTS) method for the modeling of the unsteady spherically propagating flames of n-decane-air mixtures. A significant increase of computation efficiency is achieved. The present method is an extension of the previous work of Ref. [13], DRG [14, 15] and DRGEP [16]

Path Flux Analysis Method

The goal of mechanism reduction is to identify species which are important to the target species. Therefore, it is crucial to define the importance index (interaction coefficient) of each species in the mechanism. In the DRG method, the direct interaction coefficient is defined as [14]:

$$r_{AB}^{DRG} = \frac{\sum_{i=1,I} \left| \nu_{A,i} \omega_i \delta_B^i \right|}{\sum_{i=1,I} \left| \nu_{A,i} \omega_i \right|} \qquad (1)$$

$$\delta_B^i = \begin{cases} 1 \text{ if the } i\text{th elementary reaction} \\ \quad \text{involves species B} \\ 0 \text{ otherwise} \end{cases}$$

$$\omega_i = \omega_{f,i} - \omega_{b,i} \qquad (2)$$

where $\nu_{A,i}$ is the stoichiometric coefficient of species A in the i^{th} reaction. $\omega_{f,i}$, $\omega_{b,i}$, and ω_i are the forward, backward, and net reaction rate of the i^{th} reaction, respectively. I is the total number of elementary reactions. The magnitude of r_{AB}^{DRG} shows the dependence/importance of species B to species A [14].

To initiate the selection process, a set of pre-selected species (e.g. A) and a threshold value ε need to be specified. If $r_{AB}^{DRG} < \varepsilon$, the relation between B and A is considered to be negligible. On the other hand, species B is selected when $r_{AB}^{DRG} \geq \varepsilon$.

However, because the direct interaction coefficient is not conservative, one drawback of this method is that only the first generation (directed relation) of the pre-selected species is considered. In the point view of reaction flux, both the first generation and the second generation or the higher generations are important.

In this study, instead of using the absolute reaction rate, we use the production and consumption fluxes to identify the important reaction pathways. The production and consumption fluxes, P_A and C_A, of species A can be calculated as following:

$$P_A = \sum_{i=1,I} max(\nu_{A,i}\omega_i, 0) \quad (3)$$

$$C_A = \sum_{i=1,I} max(-\nu_{A,i}\omega_i, 0) \quad (4)$$

And the flux of species A related with species B can be calculated as

$$P_{AB} = \sum_{i=1,I} max(\nu_{A,i}\omega_i\delta_B^i, 0) \quad (5)$$

$$C_{AB} = \sum_{i=1,I} max(-\nu_{A,i}\omega_i\delta_B^i, 0) \quad (6)$$

Here P_{AB} and C_{AB} denote, respectively, the production and consumption rates of species A due to the existence of species B.

In order to consider the conservative flux information, we introduce a different definition of the interaction coefficients, which contain the flux information for both the first and second generation. Note that although in the present studies, only two generation fluxes are considered, the method can be extended to any generations. Nevertheless, with the increase of the number of generations, the computation time is proportional to (species number) $^{\text{generations}}$.

The interaction coefficients for production and consumption of species A via B of first generation are defined as:

$$r_{AB}^{pro-1st} = \frac{P_{AB}}{\max(P_A, C_A)} \quad (7)$$

$$r_{AB}^{con-1st} = \frac{C_{AB}}{\max(P_A, C_A)} \quad (8)$$

By using the production and consumption fluxes of the first generation, The interaction coefficients which are the measures of flux ratios between A and B via a third reactant (M_i) for the second generation are defined as:

$$r_{AB}^{pro-2nd} = \sum_{M_i \neq A,B} (r_{AM_i}^{pro-1st} r_{M_iB}^{pro-1st}) \quad (9)$$

$$r_{AB}^{con-2nd} = \sum_{M_i \neq A,B} (r_{AM_i}^{con-1st} r_{M_iB}^{con-1st}) \quad (10)$$

The summation here includes all possible reaction paths (fluxes) relating *A* and *B*.

In theory, different threshold values can be set for different interaction coefficients. For simplicity, we can lump all the interaction coefficients together and set only one threshold value,

$$r_{AB} = r_{AB}^{pro-1st} + r_{AB}^{con-1st} + r_{AB}^{pro-2nd} + r_{AB}^{con-2nd} \quad (11)$$

The coefficient defined above is used to evaluate the dependence/importance of species *B* to species *A* in the present study.

To demonstrate the strategy of the present model, a schematic of flux transfer between *A* and *B* via other reactants (M_i) is depicted in Fig. 1.

Suppose species *A* is a pre-selected reactant (the target), and M_1 to M_8 are the intermediate species which connect species *A* with products *B*, *C*, *D*, *X* and *Y*. For the sake of simplicity of analysis, one can assume no accumulation of the intermediate species. The values on the arrows are the ratios of the flux of species *A* to each product (i.e. the percentage of species *A* changed to other species). Let us assume our goal is to select 5 or 6 species to construct a reduced mechanism from the above diagram. In order to do so, for the DRG method, the threshold value should be ε=0.205 and species M_5 to M_8, *C* and *D* are the selected 6 species (M_5 and M_6 are selected first; and then from M_5 and M_6, M_7 and M_8 are selected; finally, from M_7 and M_8, *C* and *D* are selected). For the DRGEP method, the threshold value should be ε=0.146 and the selected species are the same with DRG method (It should be noted that DRGEP does not do iteration during the selection process. The selection process for DRGEP is that M_5 and M_6 are selected through their direct relations with species *A*. Then M_7 and M_8 are selected through indirect relations via M_5 and M_6, respectively. Finally, *C* and *D* are selected via intermediate species M_5 and M_7, M_6 and M_8, respectively). For the PFA method, the threshold value should be ε=0.215

and species M_1 to M_4, and B are the selected 5 species (for simplicity, PFA only chooses 5 species here. First species B is selected through the indirect relation via intermediate species M_1 to M_4 and then from B, the intermediate species are identified). Simple calculations can show that both DRG and DRGEP only capture 29.4% target flux, but PFA can capture 66.4% target flux. The above analysis is just one example. Similar results can be observed from many other cases and we will not list them in this paper. The important thing is that a reduction scheme which has more accurate representation of the species flux will lead to a better reduced mechanism.

In addition, from the demonstration in Fig. 1, it is also seen that the interaction coefficient defined in PFA is conservative (the interaction coefficient of two species is equal to the ratio of the flux between these two species). To give an example, let us pick up one reaction path, A-M_1-B and assume this is the only reaction path in the mechanism that is related with A and B. Consider the following two possible cases, one is that only part of species A are converted to B through M_1 and the other is all species A are converted to B through M_1.

Case 1: at a specific time interval, 100 units of species A change to M_1, and at the same time, 99 units of species M_1 are converted to B, and this is the only reaction path of species M_1. It is obvious that the flux from A to B is 99 units. We can calculate the flux ratio using our definition in Eq. 10 as the following.

$$r_{AB}^{pro-2nd} = \frac{C_{AM_1}}{\max(P_A, C_A)} \times \frac{C_{M_1B}}{\max(P_{M_1}, C_{M_1})} = \frac{100}{100} \times \frac{99}{100} = 99\% \qquad (12)$$

Therefore, our flux definition also gives the same 99% flux of species A changing to species B. This agreement implies that the definition of our present second generation interaction coefficient (flux ratio) is physically meaningful.

Case 2: at a specific time interval, 100 units of species A change to M_1, and at the same time, 101 units of species M_1 change to B and this is the only reaction path of species M_1. The overall

reaction flux from *A* to *B* is 100 units. By using our definition in Eq.10, we can calculate the flux ratio as the following.

$$r_{AB}^{pro-2nd} = \frac{C_{AM_1}}{\max(P_A, C_A)} \times \frac{C_{M_1B}}{\max(P_{M_1}, C_{M_1})} = \frac{100}{100} \times \frac{101}{101} = 100\% \qquad (13)$$

The predicted results are also in consistent with the real flux from species *A* to species *B*. This above comparison also clarifies the physical meaning of the present definition of interaction coefficient (flux ratio). Therefore, in both Case 1 and Case 2, PFA gives correct indirect interaction coefficients between two correlating species. Similar results can be obtained for other multi-reaction paths. Therefore, compared to DRG and DRGEP, the present PFA method is more accurate to reproduce the reaction path flux and to develop a reduced mechanism and reaction paths based on more rigorous flux analysis.

Results and Discussion

1. Generation of reduced mechanisms for combustion of n-decane and n-heptane/air mixtures

To evaluate the PFA method, ignition delay time, the extinction curves in a perfectly stirred reactor of n-decane and n-heptane-air mixtures are examined by using the high temperature n-decane mechanism with 121 species [20, 21] and the PRF (primary reference fuel) mechanism with 116 species [21]. Both PFA and DRG are used to generate reduced mechanisms at a similar size and compared with the detailed mechanisms. For n-decane, the reduced mechanisms generated by PFA and DRG have, respectively, 54 and 55 species (further reduction will reach the limit of the methods). For n-heptane, the reduced mechanisms generated by PFA and DRG both have 56 species. In the generation of reduced mechanisms, the pre-selected species in both PFA and DRG are n-decane or n-heptane, oxygen, and nitrogen. The ignition delay time of homogeneous mixtures and the extinction curves in a perfectly stirred reactor are computed, respectively, by using the reduced mechanisms generated from PFA and DRG.

For the ignition test, SENKIN [22] is used to calculate the homogeneous ignition delay time at constant pressures. The initial mixture equivalence ratios are 0.5, 1, and 2, pressures are 1 and 20 atmospheres, and temperatures are varied between 1200 and 1700 K. For all calculations, the ignition delay time is defined as the time when the temperature increases 400 K from the initial temperature. For the PSR simulations, the inlet temperature is 500 K and the reactor pressures are changed from 1 to 20 atmospheres.

The ignition delay times and the PSR temperature dependence on flow residence time predicted by detailed mechanism and the reduced mechanisms for n-decane are compared in Fig. 2 and Fig. 3, respectively. It is clearly seen that with even a smaller number of species in the reduced mechanism generated by PFA, the results are much more accurate than that generated by DRG, particularly at lower temperatures and high pressures for ignition and lean and rich conditions for PSR. Similar results are also observed for n-heptane ignition and extinction. The ignition delay times for n-heptane are shown in Fig. 4. Again, the reduced mechanism generated by PFA reproduces accurately the ignition delay time and PSR temperature dependence from the detailed kinetic mechanism. However, the discrepancy of DRG increases at lower temperatures in a broad range of pressures.

To demonstrate that the improvement of PFA over DRG is not for a particular size of reduced mechanism, Fig. 5 shows the relations between the number of species in the reduced mechanisms of n-decane and the discrepancies of ignition delay time predicted by DRG and PFA methods at 1200 K, 1 and 20 atmospherics. It is seen that PFA improved the prediction accuracy significantly in a broad range of species numbers especially when the number of species in the reduced mechanism is less than 73. Therefore, the improvement of PFA in generating reduced mechanism is consistent with our flux analysis and is originated from the better prediction of species fluxes.

2. Reaction path flux analysis

The above ignition and PSR temperature dependence results showed that the reduced mechanism generated by PFA (with $\varepsilon = 0.47$) can reproduce the detailed mechanism much better than DRG (with $\varepsilon = 0.265$). In order to understand the difference in the accuracy of reduced mechanisms, it will be interesting to examine the impact of species selection on reaction path flux by DRG and PFA. In the two reduced mechanisms for n-decane, most of the species are the same, however, PFA selected some intermediate species such as $C_{10}H_{21}$-2, $C_{10}H_{21}$-3, $C_{10}H_{21}$-4, $C_{10}H_{21}$-5, C_4H_9, C_3H_6, but DRG chose species such as C_9H_{19}-1, C_9H_{19}-5. Are the species chosen by PFA more important? In order to answer this question, the process where these species are selected should be examined. For example, in the homogeneous ignition problem, at P =1 atm, $\tau = 4.67\times10^{-5}$ s, T=1197 K, the reaction path of n-decane is shown in Fig. 6. The numbers on the arrows in Fig. 6 denote the ratios of flux of that species from Eq. 10. We can see that $C_{10}H_{22}$ was first converted to $C_{10}H_{21}$-2, $C_{10}H_{21}$-3, $C_{10}H_{21}$-4 and $C_{10}H_{21}$-5 through H abstraction reactions. Then, these species were changed to small species C_4H_9 and C_3H_7. Even though the flux to each species which is the product of *H* abstraction reaction is not significant (that is why DRG fails to identify these intermediate species), simple calculations show that about 60% of the n-decane decomposes through these abstraction reactions and then decomposes to C_4H_9 and C_3H_7 via beta scission. Since PFA considers indirect reaction pathways, by starting from the fuel, C_4H_9 and C_3H_7 were selected and then the intermediate species ($C_{10}H_{21}$-2, $C_{10}H_{21}$-3, $C_{10}H_{21}$-4 and $C_{10}H_{21}$-5) were captured. As a result, at least 60% of the fuel flux was captured by PFA at that point. This real example also confirmed the schematic theoretical example which we presented in Fig. 1. Since the H abstraction reaction becomes more important at lower flame temperatures, the discrepancy between the reduced mechanism and the detailed mechanism will increase at lean and rich conditions without considering these reactions and their related species.

Another issue which we argued above is that an important property of a mechanism reduction model is to capture the catalytic species which have a relatively small net reaction path flux. For

example, the two catalytic species (*A* and *B*) in the following two reactions with both large comparable reaction rates are important to the oxidation of M_i but have small net reaction flux.

$$A + M_1 \rightarrow C + B \qquad (14)$$

$$B + M_2 \rightarrow C + A \qquad (15)$$

As a result, the concentrations of *A* and *B* don't change significantly. A typical example of these reactions are the catalytic effect of NO/NO_2 in the ignition of hydrocarbon fuels [17]. To make the analysis simple, one can assume *A* and *B* which form the catalytic cycle are only involved in reaction (14) and (15) which have almost the same reaction rate (P_A=C_A). Species M_1 (and M_2) have very large production rates (P_{M_1}) from other reactions. Under the definition of interaction coefficient of DRGEP [16] as described below:

$$r_{AB}^{DRGEP} = \frac{\left|\sum_{i=1,I} \nu_{A,i}\omega_i \delta_B^i\right|}{\max(P_A, C_A)} \qquad (16)$$

$$r_{AB,p} = \prod_{i=1}^{I-1} r_{M_i M_{i-1}} \qquad (17)$$

$$R_{AB} = \max_{\text{all paths p}} r_{AB,p} \qquad (18)$$

Where *p* means different reaction paths, M_i, M_{i-1} are different intermediate species. The final interaction coefficient is R_{AB}, the maximum value of the product of interaction coefficients for all possible reaction paths. Simple calculations can show that the direct interaction coefficient for *A* and *B* is zero.

$$r_{AB}^{DRGEP} = \frac{\left|P_{AB} - C_{AB}\right|}{\max(P_A, C_A)} = 0 \qquad (19)$$

The interaction coefficients for A and B through intermediate species C is also zero because r_{AC} is zero like r_{AB}.

The interaction coefficients for A and B through intermediate species M_1 (or M_2) is

$$r_{AB,1} = r_{AM_1} \times r_{M_1B} = \frac{C_{AM_1}}{\max(P_A, C_A)} \times \frac{C_{M_1B}}{\max(P_{M_1}, C_{M_1})} = \frac{C_A}{C_A} \times \frac{C_{M_1B}}{P_{M_1}} \approx 0 \qquad (20)$$

It is obvious that the interaction coefficient between *A* and *B* given by DRGEP is nearly zero and the catalytic effect which is very important may not be identified. However, as shown below, by using the present production and consumption fluxes, the PFA method can capture this important path effectively.

As an example, PFA was applied on the ignition S-curve calculation of plasma assisted methane ignition (GRI-3.0 [23]) in Ref. [17] to identify the important reaction paths. The S-curve was shown in Fig. 9 in Ref. [17] and reproduced here as Fig. 7 (b). The temperature is 900 K. The reaction path analysis of the fuel at the highest temperature position between the two counterfow burners is shown as Fig. 7 (a). The catalytic effect of NO/NO_2 can be easily captured. The direct interaction coefficient between NO and NO_2 is about 0.99 and this means that the major reaction path for NO and NO_2 are the catalytic reaction cycle. The addition of NO can change the reaction path significantly through reaction (21)-(24) to change the fairly inactive CH_3O_2 and HO_2 to active radicals. PFA showed clearly that after the addition of NO, the dominant reaction path for CH_3O_2 is reaction (21). The introduction of NO_2 also added another reaction channel for CH_3 and CH_3 was oxidized to CH_3O by reaction (22).

$$CH_3O_2 + NO \rightarrow CH_3O + NO_2 \qquad (21)$$

$$CH_3 + NO_2 \rightarrow CH_3O + NO \qquad (22)$$

$$HO_2 + NO \rightarrow OH + NO_2 \qquad (23)$$

$$H + NO_2 \rightarrow OH + NO \qquad (24)$$

The reaction path of reaction (23)-(24) is not shown in Fig. 7, but PFA showed about 40%-50% NO (vary with positions) were consumed by reaction (23) which agrees well with the results in Ref. [17]. Note that DRG will capture the same species as PFA because GRI-3.0 is a small

mechanism which does not have many parallel reaction pathways. However, the interaction coefficients of DRG do not provide any physical information of the species flux other than relation factor.

3. Modeling of steady and unsteady flame propagations using reduced mechanisms

To further verify the mechanism generated by PFA, the reduced mechanisms for n-decane and n-heptane are used to simulate the one-dimensional, quasi-steady freely propagating planar flames, and the unsteady outwardly propagating spherical flames via PREMIX [24] and A-SURF (an adaptive simulation of unsteady reactive flow code developed at Princeton University) [25, 26], respectively. The laminar flame speeds predicted by the detailed and reduced mechanisms are shown in Figs. 8 and 9. The initial temperature and pressure of the pre-mixtures are 500 K and 1 atm, respectively.

It is seen that the prediction from reduced mechanisms generated by PFA and DRG agrees well with that from the detailed chemistry, although some small deviations exist on fuel rich side. The mechanisms generated by PFA also showed better predictions especially for fuel lean case. In order to see more detailed information of the prediction by reduced models, the temperature and species distributions are examined for stoichiometric n-decane and air mixture flame, as shown in Figs. 10 and 11.

We can see the distribution of temperature and the mole fractions of major species such as $C_{10}H_{22}$, O_2, CO, and CO_2 predicted by the reduced mechanisms are exactly the same as that of the detailed mechanism. For intermediate species, Fig.11 shows that the deviations of the species profiles for the reduced mechanism generated by DRG are larger than that of PFA for CH_2O, CH_3 and HO_2. This may explain the better reproduction of the flame speeds calculated by the mechanism generated by PFA.

In order to examine the effect of unsteadiness and diffusion transport of flame propagation on the validity of reduced kinetic mechanism, the reduced and detailed models are used to simulate unsteady outwardly propagating spherical flames for n-decane/air mixtures. If ignition is initiated by a hot spot in the center of the flame and the flame will propagate outwardly spherically. Figures 12 and 13 showed the relations of spherical flame front location with time and the flame propagating speed with flame front location with different equivalence ratios. It is seen that the reduced mechanisms work extremely well for most of the cases and that the reduced model generated by PFA still works better than DRG. For the lean case (equivalence ratio = 0.7) where the mechanism generated by DRG has large deviations, the mechanism generated by PFA can still have a very good prediction of the detailed mechanism.

4. Analysis of error propagation in PFA method

From the aforementioned comparisons and applications we can see that the mechanisms generated by PFA can reproduce the results of detailed mechanisms successfully. It is also very important to examine the propagation of the errors introduced by the mechanism reduction. The errors will be introduced by removing the species and eliminating the reaction pathways in the detailed mechanism. In this section, the errors introduced by the mechanism reduction will be analyzed at different reduced mechanism sizes (different reduction levels).

The averaged error introduced by mechanism reduction of PFA method on the computation of ignition delay times as a function of threshold value are shown in Fig. 14. The computation was conducted for one atmosphere stoichiometric n-decane/air mixture from 1200 K to 1700 K. We can see in Fig. 14 that, with the increase of the threshold value of the PFA method (decreased number of species in the reduced mechanism), the averaged error increases. When the threshold value is larger than 0.65 (the number of species in the reduced mechanism is less than 43), a significant error will be introduced and the mechanism will fail to reproduce the ignition delay times. Similar phenomena were observed in the DRG method. When the threshold value is less

than 0.2, the error introduced by the reduction is small (compared to the experimental uncertainty). However, when the threshold value is larger than 0.2 (the number of species in the reduced mechanism is less than 74), significant computation error is observed. A further examination of the reduced mechanism showed that, at this threshold several important species such as C_2H_3CHO, C_3H_5O were removed by the DRG method. Because numerical simulations are mainly limited by the number of species in the reduced mechanism, the corresponding number of species in the reduced mechanisms as a function of threshold value was also shown in Fig. 14. As the number of species in the reduced mechanism decreases, the introduced error in ignition delay time increases. With the same number of species in the reduced mechanism, the mechanism generated by PFA always has a better prediction accuracy than the one generated by DRG. As we see in Fig. 14, when the number of species was less than 74, the mechanism generated by DRG introduced a significant error (20%) indicating that some important species were removed. However, for the PFA method, the error remained to be small (compared to the experimental uncertainty) until the number of species was less than 43. Therefore, the PFA method has better prediction of the important pathways than the DRG method.

In order to demonstrate the accuracy of PFA to reproduce the reaction fluxes, PFA are compared with DRG at a comparable size of the reduced mechanism for the ignition delay time and an important path flux from n-decane to C_5H_{11}-1. The reduced mechanisms generated by PFA and DRG contained 54 and 55 species, respectively. Note that at this reduction level, the error of PFA in the prediction of the ignition delay time is about 10%, which is well below the uncertainty of the experimental data [21]. The evolution of temperatures and flux ratios of the fuel molecule, $C_{10}H_{22}$ to one of its fragments, C_5H_{11}-1 calculated by the detailed mechanism, and the reduced mechanisms generated by PFA and DRG are shown in Fig. 15. We can see the predicted temperature profiles are nearly identical for the detailed mechanism and the reduced mechanism generated by PFA, even though the flux ratios from $C_{10}H_{22}$ to C_5H_{11}-1 are deviated

up to 20% between detailed and reduced mechanisms. However, the mechanism generated by DRG method predicted large derivation in temperature history and the flux ratio. Similar results were also observed for other important pathways. Therefore, in limiting cases PFA has a better prediction of the important reaction fluxes than DRG.

One thing should be pointed out is that the PFA method is based on reaction path analysis. Target species which have weak chemical coupling (flux) to the pre-selected species may not be captured. One example is the NO_x formation problem. PFA will remove NO_x species because of the weak flux pathway from the oxidizer to NO_x. However, this weakness can be fixed by choosing NO, NO_2 or N_2 as a pre-selected species when NO_x formation is an important target.

Finally, the error introduced by the mechanism reduction is also examined in the computation of laminar flame speeds. Figure 16 shows the laminar flame speeds of stoichiometric n-decane/air mixture at 500 *K* and 1 *atm* as a function of different reduction levels. It is interesting that the errors introduced by mechanism reduction at different reduction levels are not monotonic with the number of species in the reduced mechanism. The errors remain small (within 4%) for all reduced mechanisms with species number larger than 50.

5. Integration of PFA with Multi-Time Scale method

To further improve the computation efficiency, the reduced mechanism is integrated with a Hybrid Multi-Time Scale method (HMTS) [27, 28]. By using the HMTS method, the computation times of ignition delays of stoichiometric n-decane/air were approximately 10% of those by using the ODE solver [29], which is used in the CHEMKIN- SENKIN [24] package. More detailed comparisons can be found in Ref. [27, 28]. In this paper, the simulation results of flame front location as a function of time for the propagating spherical stoichiometric n-decane/air flame are compared by using the ODE solver [29] and the HMTS method. It is clearly seen from Fig. 17 that the results computed by the ODE solver and the HMTS method agree very

well. By integrating the reduced mechanism and HMTS method, a significant increase of computation efficiency is observed. The results suggest that the integration of the dynamic multi-timescale (MTS) model with the PFA mechanism reduction approach is promising to increase dramatically the computation efficiency in the direction numerical simulations involving large kinetic mechanisms.

Conclusion

A path flux analysis method to generate reduced mechanisms is presented and validated. The methodology extends the effectiveness of the existing DRG method and can identify the important multi-generation pathways and species in catalytic cycles. Different sized reduced mechanisms for n-decane and n-heptane ignition, extinction, and steady and unsteady flame propagation are generated and examined. Comparison between the present PFA method and the DRG method for ignition and flame propagation show that with the same or smaller sized reduced mechanisms, PFA has better accuracy than DRG to reproduce ignition and extinction of n-decane and n-heptane mixtures in a broad temperature and pressure range. The simulation of unsteady spherical flame initiation process demonstrates that the PFA generated reduced mechanism also work well for unsteady combustion processes involving non-equilibrium flame structures and diffusion transport. A further increase of computation efficiency is achieved by the integration of the PFA method and the multi-timescale method for the detailed modeling of n-decane and n-heptane flames.

Acknowledgement

This work is supported by the MURI project supported by the Air Force Office of Scientific Research (AFOSR) under the guidance of Dr. Julian Tishkoff and by the DoE University Coal Research Program.

References

[1] N. Peters, Lecture Notes in Physics, Springer, Berlin, Germany, 1987.

[2] J.Y. Chen, Combust. Sci. Technol. 57 (1988) 89-94.

[3] Y. Ju, T. Niioka, Combust. Flame. 99 (1994) 240-246.

[4] S.H. Lam, Combust. Sci. Technol. 89 (1993) 375-404.

[5] A. Massias, D. Diamantis, E. Mastorakos, D.A. Goussis, Combust. Flame. 117 (1999) 685-708.

[6] T. Lu, Y. Ju, C.K. Law, Combust. Flame. 126 (2001) 1445-1455.

[7] U. Maas, S.B. Pope, Combust. Flame. 88 (1992) 239-264.

[8] S.B. Pope, Combust. Theory Model. 1 (1997) 41-63.

[9] S.R. Tonse, N.W. Moriarty, M. Frenklach, N.J. Brown, Int. J. Chem. Kinet. 35 (2003) 438-452.

[10] G. Li, H. Rabitz, J. Hu, Z. Chen, Y. Ju, J. Math. Chem. 43 (2008) 1207-1232.

[11] T. Turanyi, Computers Chem. 18 (1994) 45-54.

[12] Y. Zhang, R. Rawat, G. Schmidt, Acceleration of detailed chemistry calculation in multidimensional engine modeling using DOLFA. International Multidimensional Engine Modeling User's Group Meeting, Detroit, MI, USA, 2005.

[13] A.B. Bendtsen, P. Glarborg, K. Dam-Johansen, Computers Chem. 25 (2001) 161-170.

[14] T. Lu, C.K. Law, Proc. Combust. Inst. 30 (2005) 1333-1341.

[15] T. Lu, C.K. Law, J. Chen, Development of Non-stiff Reduced Mechanisms for Direct Numerical Simulations, in: 46th AIAA Aerospace Sciences Meeting and Exhibit including The New Horizons Forum and Aerospace Exposition, Reno, NV, USA, 2008.

[16] P. Pepiot, H. Pitsch, Combust. Flame. 154 (2008) 67-81.

[17] T. Ombrello, Y. Ju, A. Fridman, AIAA J. 46 (2008) 2424-2433.

[18] Y. Xin, C.K. Law, T. Lu, A Reduced Mechanism for iso-Octane Oxidation, in: 6th US National Combustion Meeting, Ann Arbor, MI, USA, 2009.

[19] K.E. Niemeyer, M.P. Raju, C.J. Sung, Skeletal Mechanism Generation for Surrogate Fuels Using Directed Relation Graph with Error Propagation and Sensitivity Analysis, in: 6th US National Combustion Meeting, Ann Arbor, MI, USA, 2009.

[20] M. Chaos, A. Kazakov, Z. Zhao, F.L. Dryer, S.P. Zeppieri, Reduced High-Temperature Mechanisms for Large Paraffins - n-Hexadecane, in: Eastern States Fall Technical Meeting of the Combustion Institute, Orlando, FL, USA, 2005.

[21] M. Chaos, A. Kazakov, Z. Zhao, F.L. Dryer, Int. J. Chem. Kinet. 39 (2007) 399-414.

[22] A.E. Lutz, R.J. Kee, J.A. Miller, SENKIN: A FORTRAN Program for Predicting Homogeneous Gas Phase Chemical Kinetics with Sensitivity Analysis, 1997.

[23] G.P. Smith, D.M. Golden, M. Frenklach, N.W. Moriarty, B. Eiteneer, M. Goldenberg, C.T. Bowman, R.K. Hanson, S. Song, W.C. Gardiner, Jr., V.V. Lissianski, Z. Qin, GRI-3.0, Http://www.me.berkeley.edu/gri_mech/

[24] R.J. Kee, J.F. Grcar, M.D. Smooke, J.A. Miller, A FORTRAN program for modeling steady laminar one-dimensional premixed flames, Sandia National Laboratory Report SAND85-8240, 1985.

[25] Z. Chen, Studies on the initiation, propagation, and extinction of premixed flames, in Mechanical and Aerospace Engineering, Ph.D. Thesis, Princeton University, USA, 2009.

[26] Z. Chen, M.P. Burke, Y. Ju, Proc. Combust. Inst. 32 (2009) 1253-1260.

[27] X. Gou, Z. Chen, W. Sun, Y. Ju, An Efficient Multi Time Scale Method for Solving Stiff ODEs with Detailed Kinetic Mechanisms and Multi Scale Physical Chemical Processes, in: 47th AIAA Aerospace Sciences Meeting including The New Horizons Forum and Aerospace Exposition, Orlando, FL, USA, 2009.

[28] X. Gou, W. Sun, Z. Chen, Y. Ju, A Dynamic Multi Time Scale Method for Modeling of Combustion with Detailed Kinetic Mechanisms, in: 6th US National Combustion Meeting, Ann Arbor, MI, USA, 2009, also submitted to Combust. Flame., 2009.

[29] P.N. Brown, G.D. Byrne, A.C. Hindmarsh, Siam Journal on Scientific and Statistical Computing, 10 (1989) 1038-1051.

List of captions for the figures

Fig. 1 Schematic of flux relation between different species

Fig. 2 Comparison of ignition delay times of lean, stoichiometric, and rich n-decane-air mixtures for various temperatures and pressures predicted by using reduced mechanisms generated by PFA and DRG as well as detailed mechanism

Fig. 3 Comparison of PSR-simulations of lean, stoichiometric, and rich n-decane-air mixtures for various temperatures and pressures predicted by using reduced mechanisms generated by PFA and DRG as well as detailed mechanism

Fig. 4 Comparison of ignition delay times of lean, stoichiometric, and rich n-heptane-air mixtures for various temperatures and pressures predicted by using reduced mechanisms generated by PFA and DRG as well as detailed mechanism

Fig. 5 Ignition delay time comparisons of detailed and reduced mechanisms with different sizes of reduced mechanisms

Fig. 6 Homogeneous ignition reaction path of n-decane at P =1 *atm*, $\tau=4.67\times10^{-5}$, T=1197 K, $\Phi=1$

Fig. 7 (a) Ignition pathway of CH_4 at the highest temperature point, (b) S-curve response for 12% CH_4 in N_2 vs preheated air with 10,000 ppm NO as a function of maximum temperature and strain rate

Fig. 8 The laminar flame speed as a function of equivalence ratio for n-decane/air mixtures at 500 *K* and 1 *atm*.

Fig. 9 The laminar flame speed as a function of equivalence ratio for n-heptane/air mixtures at 500 *K* and 1 *atm*.

Fig. 10 Temperature and major species profiles for a stoichiometric n-decane/air mixture at 500 *K* and 1 *atm*

Fig. 11 Species profiles for a stoichiometric n-decane/air mixture at 500 *K* and 1 *atm*

Fig. 12 Flame front location as a function of time for propagating spherical n-decane/air flames.

Fig. 13 Flame propagating speed of burned gas as a function of flame front location for propagating spherical n-decane/air flames.

Fig. 14 Averaged error of ignition delay predicted by reduced mechanisms and the number of species in the reduced mechanism as a function of the threshold value for a stoichiometric n-decane/air mixture at 1 *atm*

Fig. 15 Temperatures and fuel decomposition flux ratios as a function of time in detailed and reduced mechanisms for a stoichiometric n-decane/air mixture at initial temperature 1200 *K* and 1 *atm*

Fig. 16 The laminar flame speed and the error predicted by the reduced mechanism as a function of number of species in reduced mechanism for a stoichiometric n-decane/air mixture at 500 *K* and 1 *atm*

Fig. 17 Flame front location as a function of time for propagating spherical n-decane/air flames by ODE and HMTS methods

Figures:

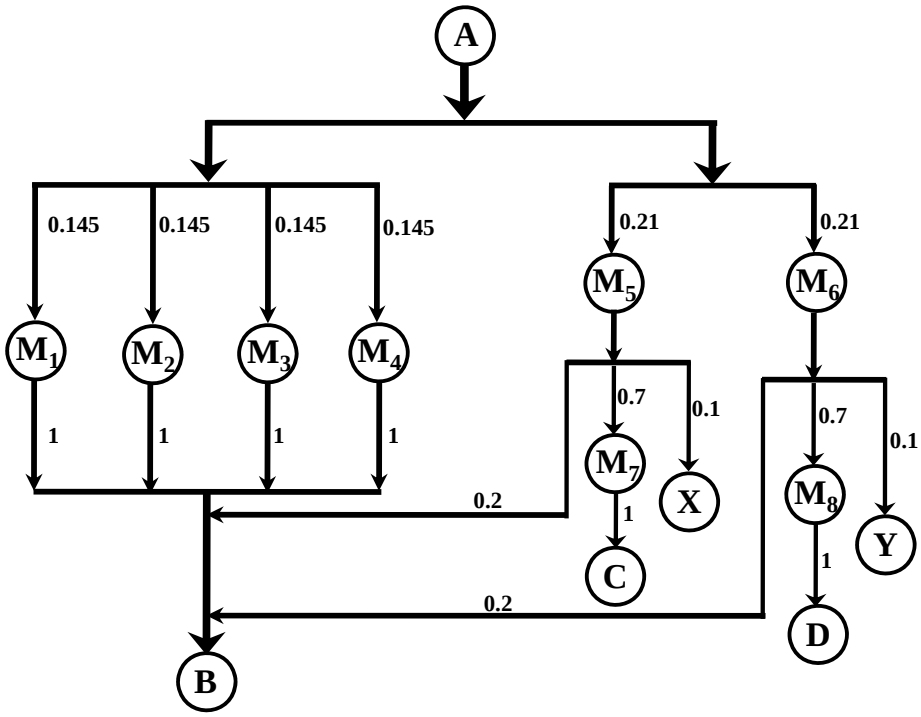

Fig. 1 Schematic of flux relation between different species

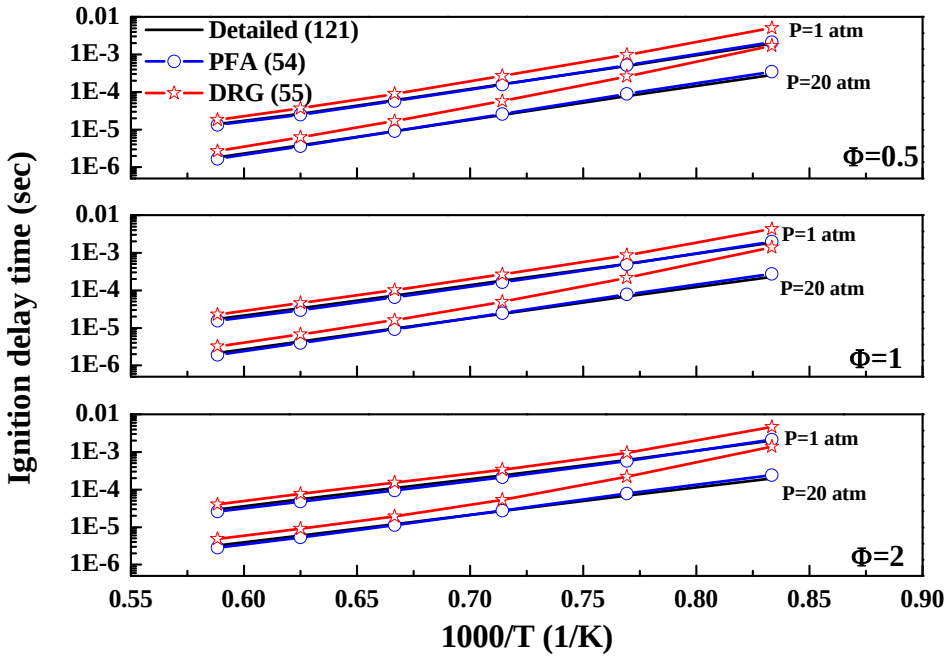

Fig. 2 Comparison of ignition delay times of lean, stoichiometric, and rich n-decane-air mixtures for various temperatures and pressures predicted by using reduced mechanisms generated by PFA and DRG as well as detailed mechanism

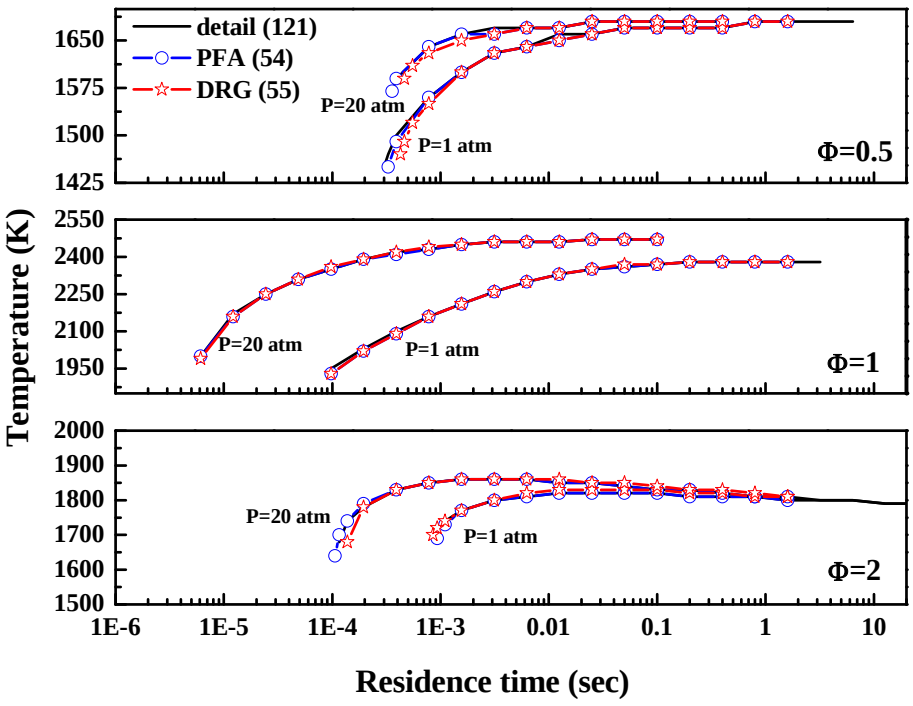

Fig. 3 Comparison of PSR-simulations of lean, stoichiometric, and rich n-decane-air mixtures for various temperatures and pressures predicted by using reduced mechanisms generated by PFA and DRG as well as detailed mechanism

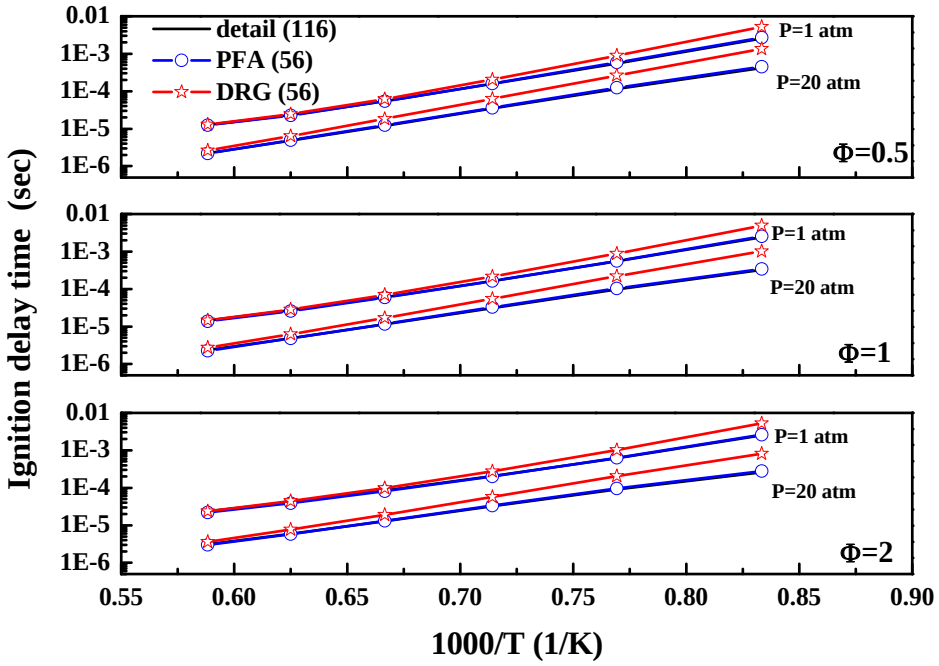

Fig. 4 Comparison of ignition delay times of lean, stoichiometric, and rich n-heptane-air mixtures for various temperatures and pressures predicted by using reduced mechanisms generated by PFA and DRG as well as detailed mechanism

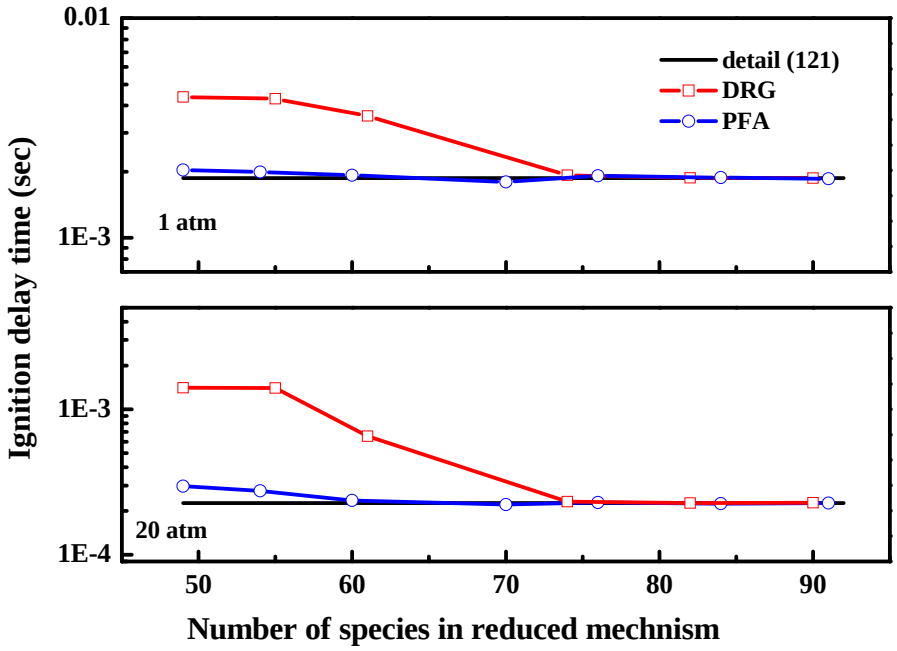

Fig. 5 Ignition delay time comparisons of detailed and reduced mechanisms with different sizes of reduced mechanisms

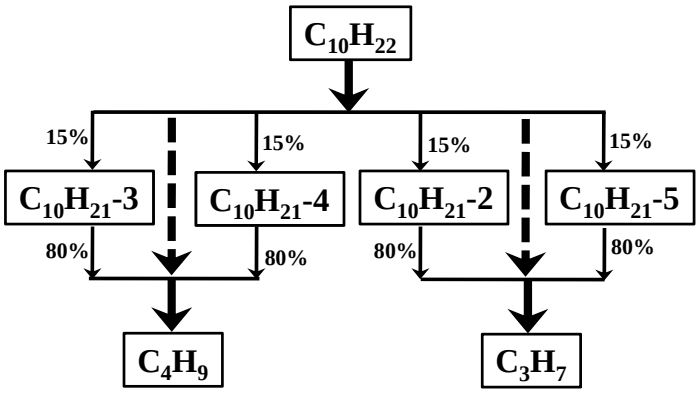

Fig. 6 Homogeneous ignition reaction path of n-decane at P =1 atm, $\tau=4.67\times10^{-5}$ s, T=1197 K, Φ=1

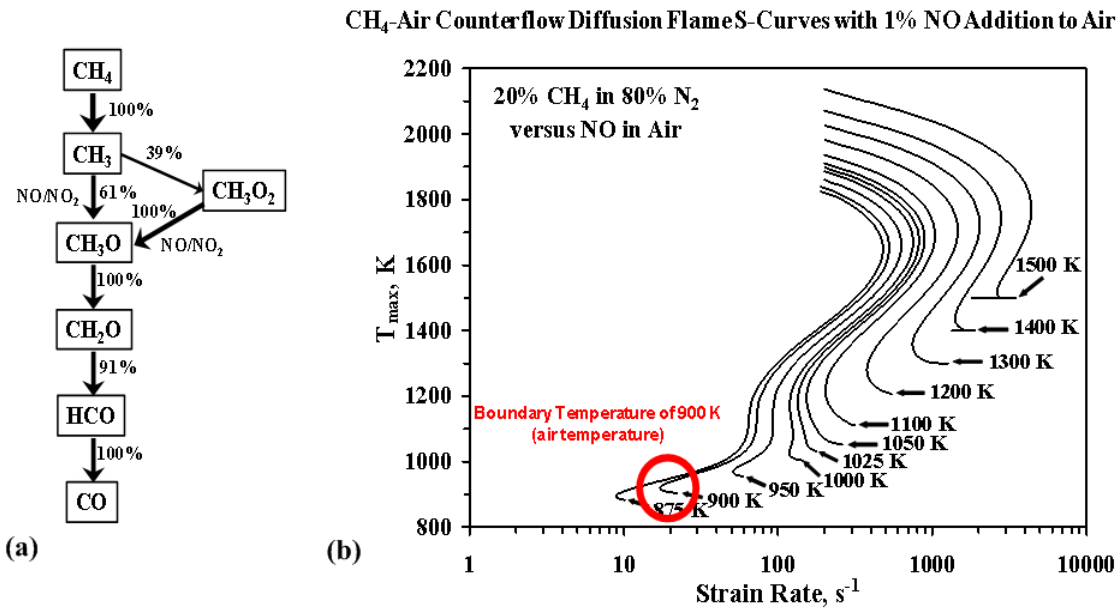

Fig. 7 (a) Ignition pathway of CH_4 at the highest temperature point, (b) S-curve response for 12% CH_4 in N_2 vs preheated air with 10,000 ppm NO as a function of maximum temperature and strain rate

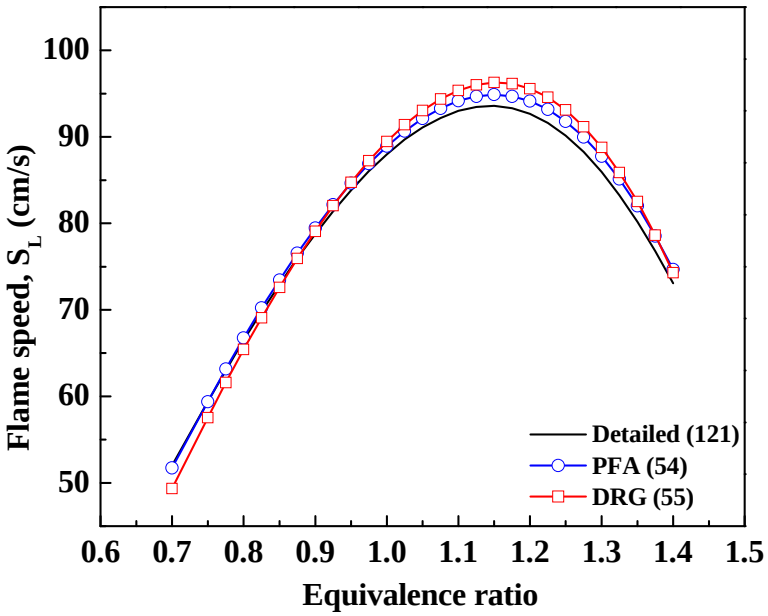

Fig. 8 The laminar flame speed as a function of equivalence ratio for n-decane/air mixtures at 500 *K* and 1 *atm*.

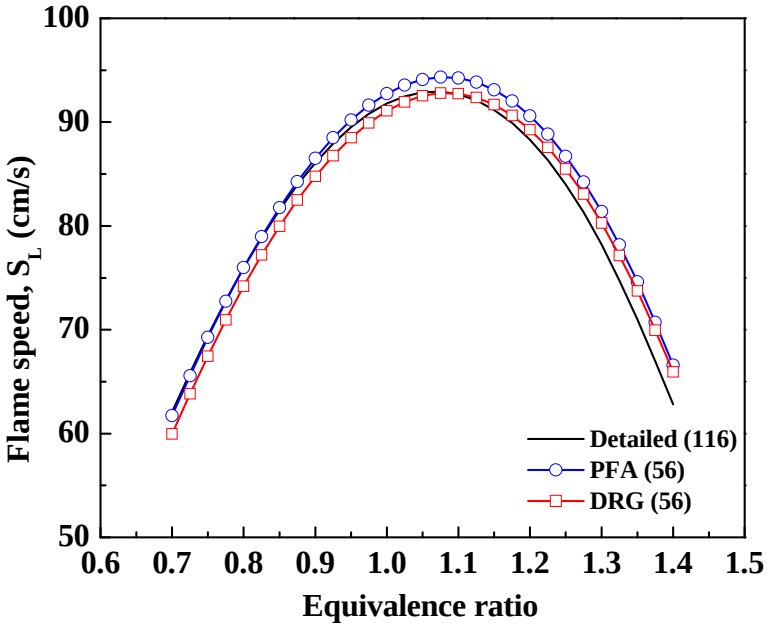

Fig. 9 The laminar flame speed as a function of equivalence ratio for n-heptane/air mixtures at 500 *K* and 1 *atm*.

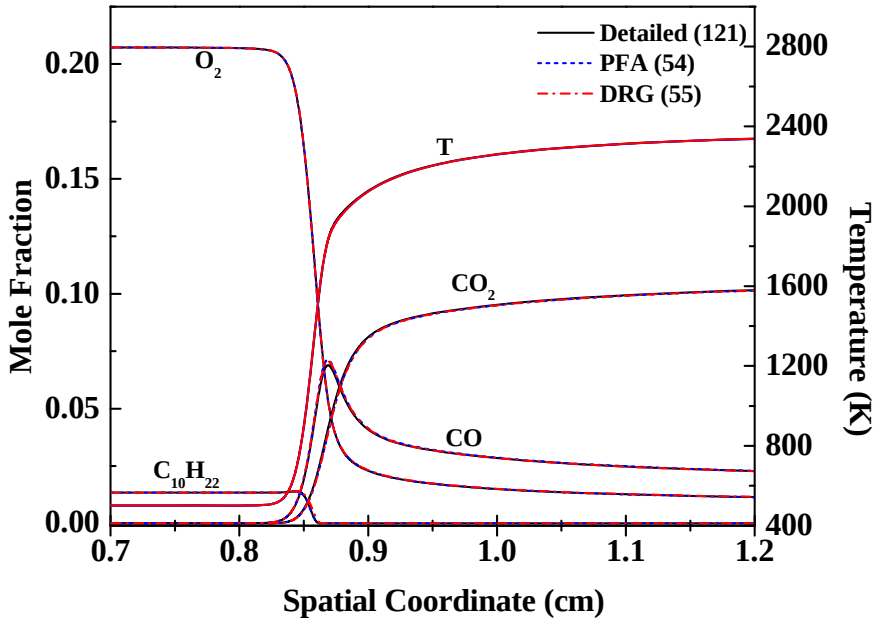

Fig. 10 Temperature and major species profiles for a stoichiometric n-decane/air mixture at 500 *K* and 1 *atm*

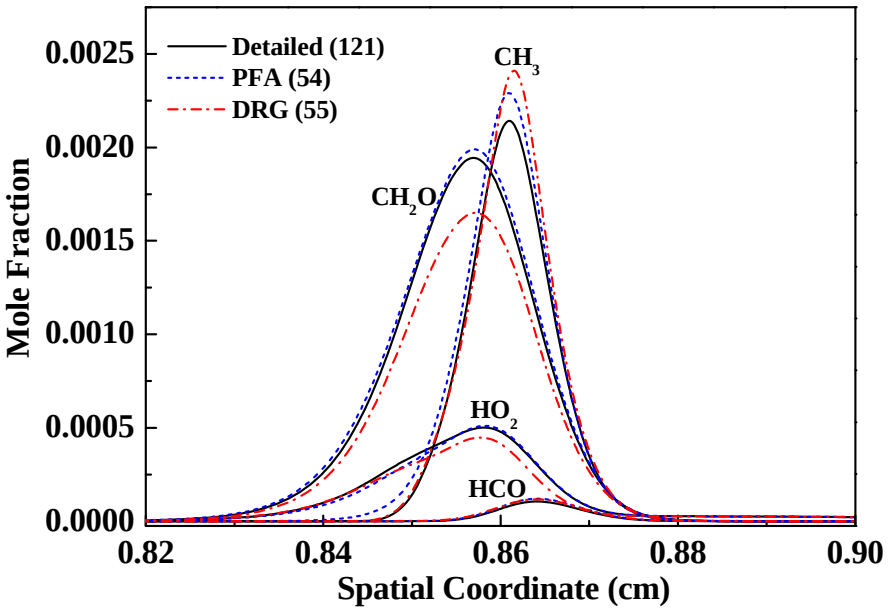

Fig. 11 Species profiles for a stoichiometric n-decane/air mixture at 500 *K* and 1 *atm*

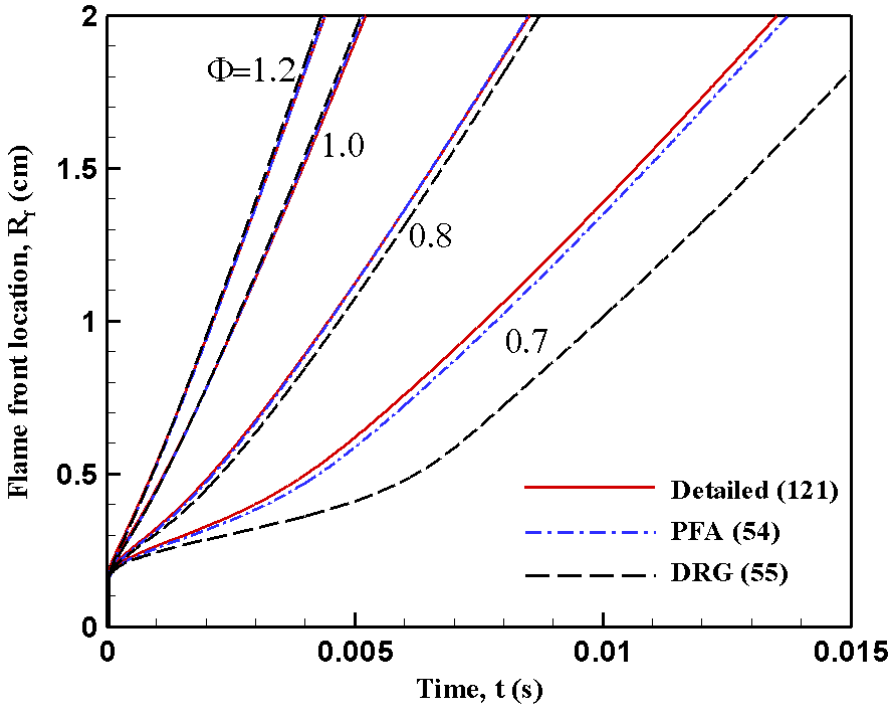

Fig. 12 Flame front location as a function of time for propagating spherical n-decane/air flames.

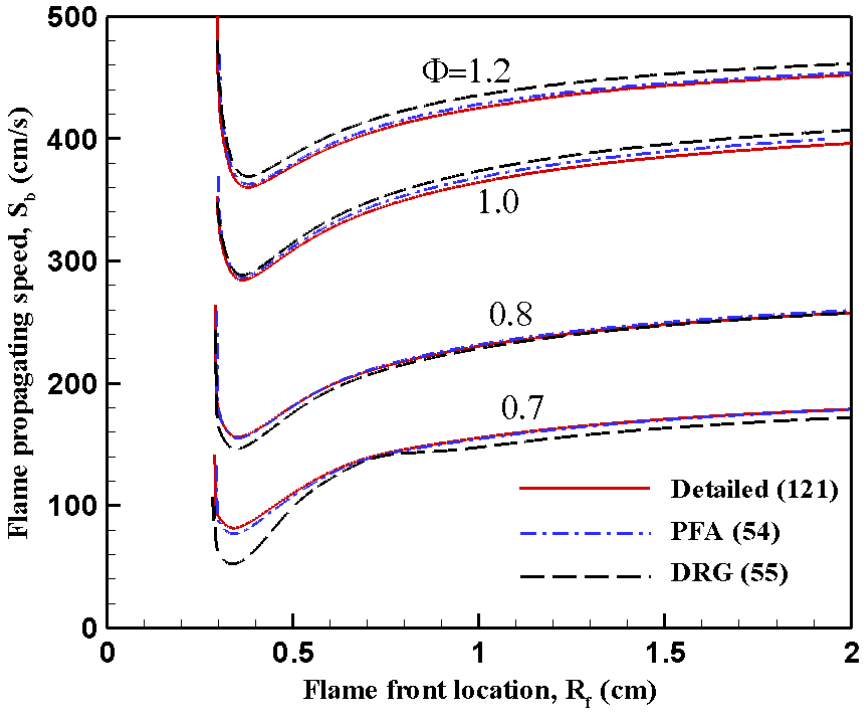

Fig. 13 Flame propagating speed of burned gas as a function of flame front location for propagating spherical n-decane/air flames.

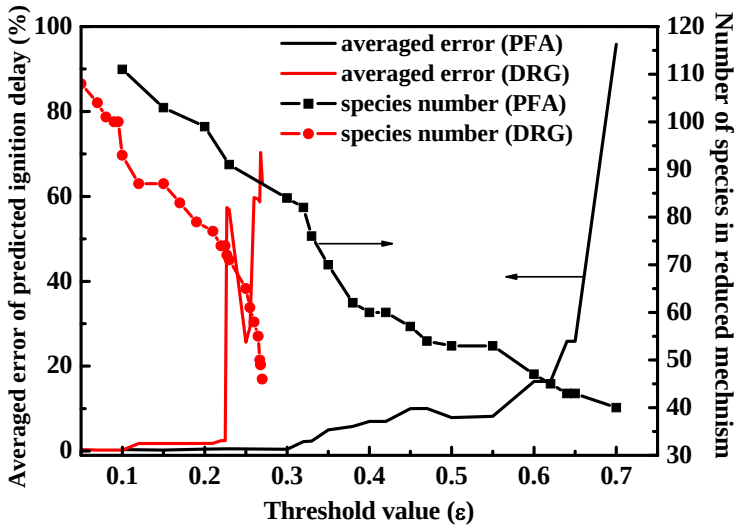

Fig. 14 Averaged error of ignition delay predicted by reduced mechanisms and the number of species in the reduced mechanism as a function of the threshold value for a stoichiometric n-decane/air mixture at 1 *atm*

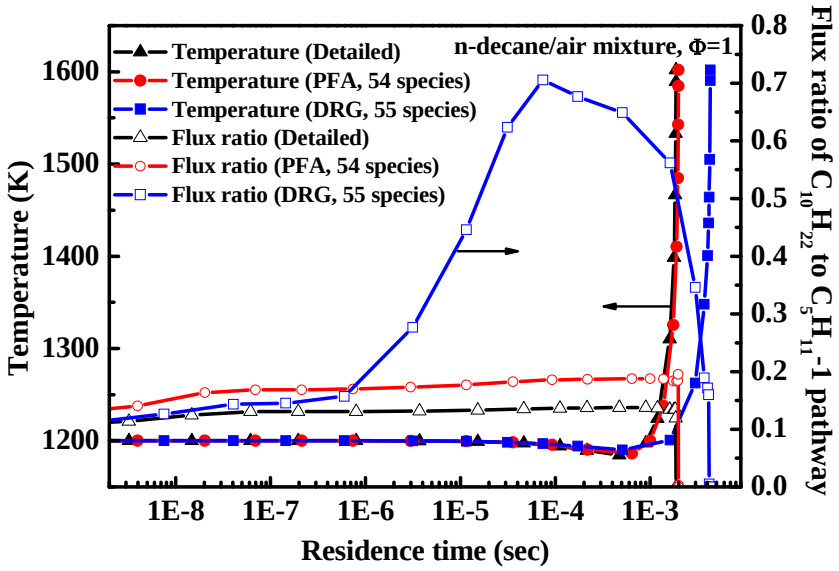

Fig. 15 Temperatures and fuel decomposition flux ratios as a function of time in detailed and reduced mechanisms for a stoichiometric n-decane/air mixture at initial temperature 1200 K and 1 *atm*

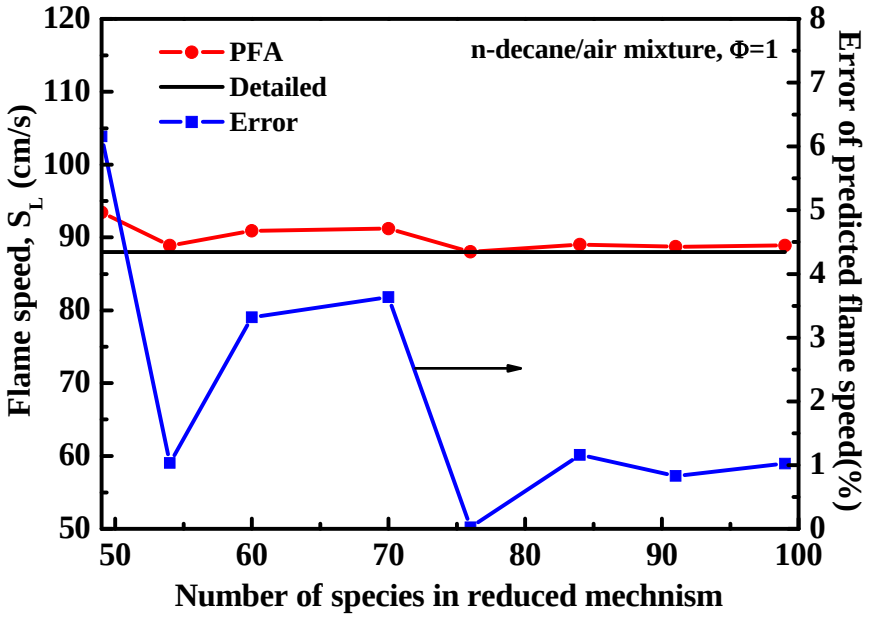

Fig. 16 The laminar flame speed and the error predicted by the reduced mechanism as a function of number of species in reduced mechanism for a stoichiometric n-decane/air mixture at 500 *K* and 1 *atm*

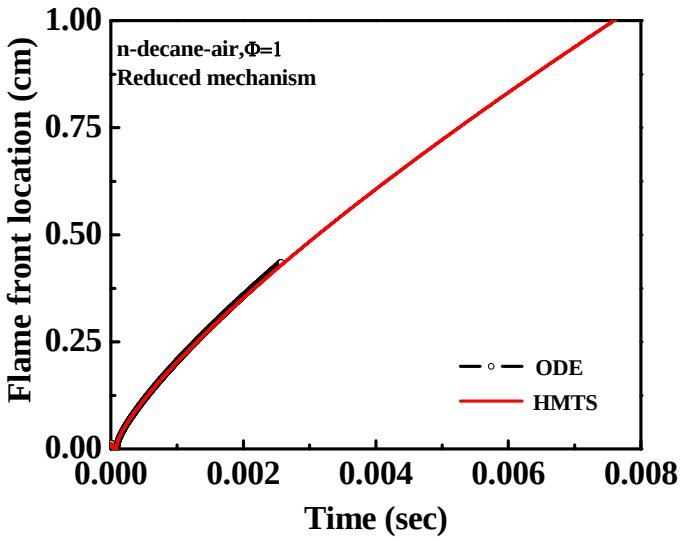

Fig. 17 Flame front location as a function of time for propagating spherical n-decane/air flames by ODE and HMTS methods